Energy Impacts of Nonlinear Behavior of PCM When Applied into Building Envelope

Preprint

P.C. Tabares-Velasco

ENERGY IMPACTS OF NONLINEAR BEHAVIOR OF PCM WHEN APPLIED INTO BUILDING ENVELOPE

Paulo Cesar Tabares-Velasco
National Renewable Energy Laboratory
Golden, Colorado, USA

ABSTRACT

Research on phase change materials (PCM) as a potential technology to reduce peak loads and HVAC energy use in buildings has been conducted for several decades, resulting in a great deal of literature on PCM properties, temperature, and peak reduction potential. However, there are few building energy simulation programs that include PCM modeling features, and very few of these have been validated. Additionally, there is no previous research that indicates the level of accuracy when modeling PCMs from a building energy simulation perspective. This study analyzes the effects a nonlinear enthalpy profile has on thermal performance and expected energy benefits for PCM-enhanced insulation. The impact of accurately modeling realistic, nonlinear enthalpy profiles for PCMs versus simpler profiles is analyzed based on peak load reduction and energy savings using the Conduction Finite Difference (CondFD) algorithm in EnergyPlus. The PCM and CondFD models used in this study have been previously validated after intensive verification and validation done at the National Renewable Energy Laboratory. Overall, the results of this study show annual energy savings are not very sensitive to the linearization of enthalpy curve. However, hourly analysis shows that if simpler linear profiles are used, users should try to specify a melting range covering roughly 80% of the latent heat, otherwise, hourly results can differ by up to 20%.

INTRODUCTION

Phase change materials (PCMs) have multiple applications for buildings such as wallboards impregnated with PCMs [1, 2], PCMs impregnated in fiber insulation, macro encapsulated PCMs in walls [3] (Kosny, Shrestha et al. 2010), floor heating systems that utilize shape-stabilized PCMs [4], or combination of different PCMs [5] among several applications previously analyzed. The flexibility of PCMs to combine in multiple applications is due to the variety of materials and thermal properties that results in a wide range of latent heat storage capacities and phase change temperatures. This flexibility combined with the high cost of PCMs results in added complexity to design the best PCM application for a particular scenario. Thus, design of PCMs is a complicated task that requires building energy simulation programs able to model PCMs for different applications in homes such as ESP-r [6-8] and TRNSYS [2, 9, 10]. EnergyPlus can simulate PCMs with the Conduction Finite Difference (CondFD) algorithm. Both of the PCM and CondFD models have been recently validated, and preliminary results showed potential energy savings when PCMs are installed in houses [5, 11, 12].

Most PCM models in energy simulation programs require knowledge of the enthalpy or specific heat as a function of temperature. In particular, PCM modeling in EnergyPlus requires input of enthalpy as a function of temperature. The enthalpy-temperature function for most PCMs is not linear and many times not known in detail. Obtaining this data could be a challenging task that requires careful calibration of instrumentation and careful selection of heating/cooling rates [13, 14].

This study investigated the impacts on the accuracy of predicted energy benefits when a linear enthalpy function is assumed for PCM distributed in insulation with a nonlinear enthalpy function. A linear function could facilitate parametric and optimization analysis as well as broad analyses that would design generic PCMs that manufacturers could later produce following specific guidelines.

ENERGYPLUS

EnergyPlus includes the CondFD model that is an implicit finite difference scheme that numerically solves the appropriate heat transfer equations. CondFD is coupled with an enthalpy-

temperature function (enthalpy curve) that users input to account for latent heat storage in PCMs as shown in Equation 1. This function is used to develop an equivalent specific heat at each time step as shown in Equation 2. This equivalent specific heat is then updated and input into the CondFD as shown in Equation 3 [15].

$$h = h(T) \tag{1}$$

$$C_p^* = \frac{h_i^j - h_i^{j-1}}{T_i^j - T_i^{j-1}} \tag{2}$$

$$C_p \rho \Delta x \frac{T_i^{j+1} - T_i^j}{\Delta t} = k_W \frac{(T_{i+1}^{j+1} - T_i^{j+1})}{\Delta x} + k_E \frac{(T_{i-1}^{j+1} - T_i^{j+1})}{\Delta x} \tag{3}$$

PROBLEM DESCRIPTION

This study simulated seven PCMs (one with realistic enthalpy profile and six hypothetical) with the same latent heat characteristics to investigate the impacts the enthalpy curve has on predicting accurate energy benefits when a linear enthalpy function is used. All PCMs have different melting ranges but are centered at the same middle melting temperature as shown in Figure 1 and Table 1. The temperature ranges of the six hypothetical PCMs were selected arbitrarily to represent several combinations of linear ranges that follow similar melting behavior of the nonlinear PCMs: from a wider range to a very narrow melting range. The PCM with a nonlinear enthalpy curve (NonLin) represents a more realistic PCM analyzed previously by a different study with a melting range of 24°-33°C where roughly 80% of the latent heat is between 29°-31.5°C [16]. In contrast, L-6 represents an ideal PCM with a fixed melting temperature. For simulation purposes, L-6 has a 0.4°C temperature range because EnergyPlus requires a temperature range for the phase change to happen. In fact, this study found that simulating PCMs with a very narrow (less than 1°C) melting range produces longer run times than when using wider melting range (4°-5°C). This is due to the additional iteration needed to converge when using narrow melting ranges.

Table 1 also shows the root mean square error (RMSE) for the enthalpy curve calculated based on the differences with the nonlinear profile. The RMSE in Table 1 is normalized by the equivalent latent heat of the PCMs. The equivalent latent heat of aggregated PCM insulation was set equal to 34 kJ/kg. This value was selected based on a previous study that looked into the same PCM application [17]. All PCMs have the same thermal properties for the liquid/solid phases and storage capacity as shown in Table 2 except for the melting range—the temperature range where phase change occurs. All PCMs shown in Table 1 were simulated using an internal version of EnergyPlus v7 with a debugged and validated PCM model that will be available in version 7.1 [5, 11]. All simulations used a 1-minute time step and have the same boundary and initial

conditions. The only difference between PCMs was the enthalpy curve. From all six hypothetical PCMs, L-4 shows the smallest RMSE, suggesting that it might be the best linear approximation to the enthalpy curve. This hypothesis is tested as the seven PCMs were compared under two different scenarios: one wall with simple boundary conditions and simple building using TMY3 weather data for Phoenix, AZ. Phoenix was selected because of large daily temperature oscillations.
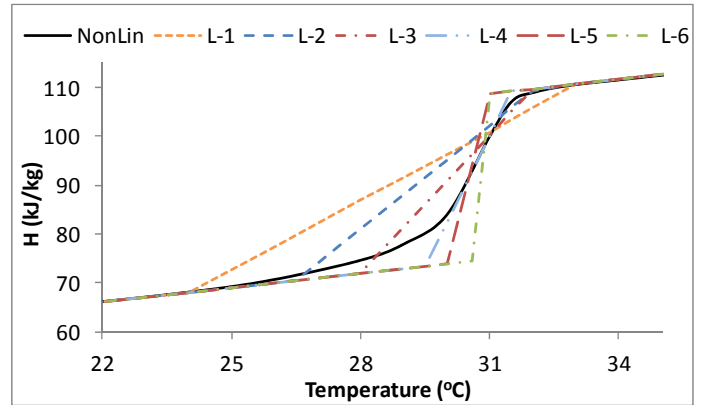
Figure 1. Enthalpy curves for PCMs analyzed as shown in Table 1

Table 1. Melting range of PCMs analyzed

PCM	Melting Range (°C)	RMSE/Latent Heat	Linear Profile
NonLin	24-33	N/A	Nonlinear
L-1	24-33	0.23	Linear
L-2	26-32	0.10	Linear
L-3	28-32	0.08	Linear
L-4	29.5-31.5	0.06	Linear
L-5	30-31	0.14	Linear
L-6	30.6-31	0.18	Linear

Table 2. PCM-Insulation Properties for Wall Tests

Variable	Value
% Weight of PCM in Insulation	20%
Equivalent Latent Heat	34 kJ/kg
Thermal Conductivity	0.0337 W/mK
Density	50 kg/m^3
Specific Heat	960 J/kg K
Thickness of PCM-Insulation	0.1m
PCM-Insulation Latent Storage	170 kJ/m^2
Amount of PCM	1 kg/m^2

WALL SUB-HOURLY ANALYSIS

The wall sub-hourly analysis consisted of a wall with: 1cm wood, 10cm fiber insulation with PCMs, and 1.5cm drywall. The outdoor boundary condition was a 24-hr sine wave test for

three identical days with amplitude of 30°C (outside temperature ranged from 10-40°C) and an outdoor convective heat transfer coefficient equal to 20W/m²K. Interior boundary conditions were set by keeping indoor air temperature equal to 25°C with an indoor convective heat transfer coefficient equal to 5W/m²K. This allowed the inside surface temperature of the wall to oscillate during the test. The wall was initially at a homogenous temperature of 25°C. A more extensive description on the numerical problem can be found in a similar case used for comparative verification purposes [11].

Figure 2 shows the temperature for the second of the three simulated days at the middle of the insulation with distributed PCM for all simulated walls with PCMs (NonLin, L-1 to L-6) and without PCMs (NoPCM). The sketch on Figure 2 shows the location of the temperature node. All simulated walls with PCMs show similar trends clearly different from the wall without PCM. However, PCMs with linear profile L-1 and L-2 shows differences from the rest of the PCMs when the wall is heating and cooling. This difference is because of the wider melting range that made these two PCMs melt and solidify earlier than the nonlinear PCM.
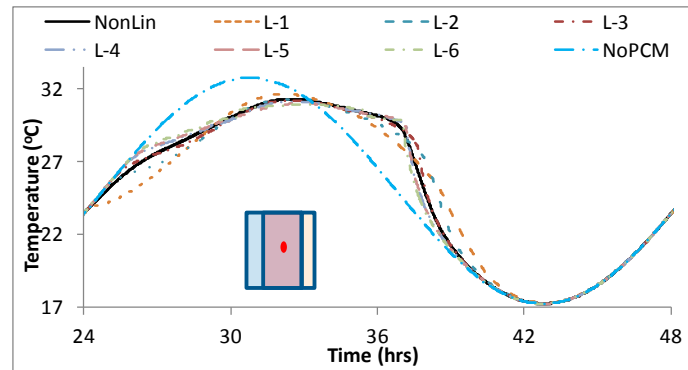

Figure 2. Calculated temperature at the middle of the insulation layer containing distributed PCM for all walls with and without PCMs

Figure 3 shows inside surface heat flux for the second day and same PCMs as in Figure 2. Figure 3 confirms that linear profiles L-1 and L-2 should not be used if the desire is to simulate a more realistic PCM with a nonlinear profile as the one chosen in this study. This selection would predict higher incoming heat fluxes to the wall because PCMs L-1 and L-2 melt earlier during the day, thus delaying the incoming heat flux earlier than the rest of the PCMs. Despite these differences, all PCM with linear profiles predicted the peak heat flux close to the nonlinear PCM.

Table 3 shows the inside net heat gain percentage differences between all linear PCM profiles and the wall without PCMs with respect to the wall with nonlinear PCM. It also shows the RMSE for the inside surface heat flux and inside surface temperature calculated based on the differences with the nonlinear profile. Highest differences are found with the

widest melting ranges—L-1 and L-2. However, these were relatively small compared to the actual difference when no PCMs are simulated. This first test shows the best linear curves for the simple boundary conditions were L-3 and L-4 and agrees with the RMSE calculated in Table 1 but in this case L-3 obtained a smaller RMSE than L-4. However, these results may vary when changing and more realistic inside and outdoor boundary conditions are used.
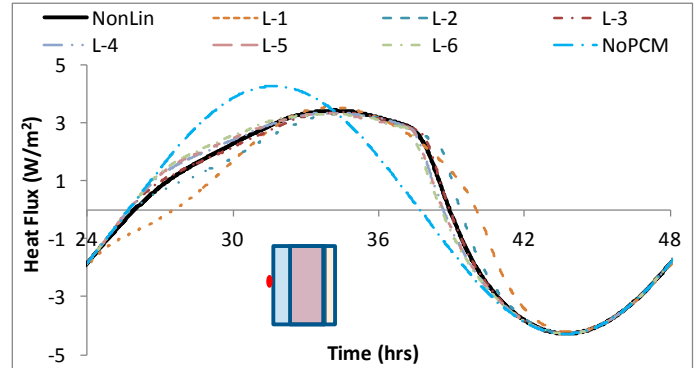

Figure 3. Calculated inside surface heat flux for the different PCMs distributed in insulation for all walls with and without PCMs

Table 3. Differences between PCMs analyzed

Melting Profile	12hr Heat Gain Difference	RMSE Inside Heat Flux (W/m²)	RMSE Inside Surface Temperature (°C)
L-1	-11.1%	0.68	0.14
L-2	-10.8%	0.36	0.07
L-3	-1.4%	0.09	0.02
L-4	4.3%	0.19	0.04
L-5	4.8%	0.21	0.04
L-6	6.9%	0.27	0.055
NoPCM	29.7%	1.015	0.2

BUILDING LEVEL ANNUAL ANALYSIS

In this study, the ASHRAE Standard 140 Case 600 model was selected to assess the impacts of enthalpy linearization due to its simplicity and because it is a well-referenced building that has been simulated by several major simulation engines (ASHRAE 2004). Figure 4 shows Case 600 building construction. The simple geometry and low internal gains make this structure more susceptible to envelope changes, a desired attribute for this study. The test building is a lightweight rectangular single zone building, with dimension of 8 m wide by 6 m long by 2.7 m high. The building has no interior partitions, a total window area of 12 m² on the south wall, and low interior gains (200 W). Moreover, the slab is highly insulated to eliminate thermal losses and gain to the ground. As mandated by ASHRAE Standard 140, the infiltration was set to 0.5 air changes per hour. Additionally, the building mechanical system is a 100% convective air ideal system with no losses or

capacity limitation. The thermostat is set with a dead band so heating takes place for temperatures below 20°C and cooling for temperatures above 27°C. Wall and roof insulation properties have been slightly modified to incorporate PCMs as described in a previous study [11]. In addition, PCMs analyzed in this section have larger latent storage than in the previous study and previous sub-hourly study as shown in Table 4.
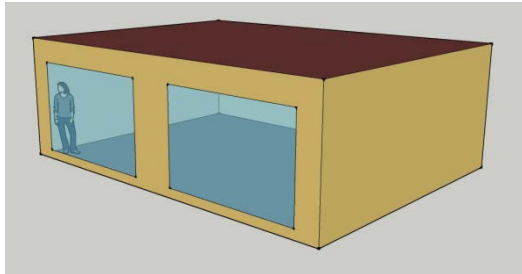

Figure 4. ASHRAE Standard 140 Case 600 construction

Table 4. PCM-Insulation Properties

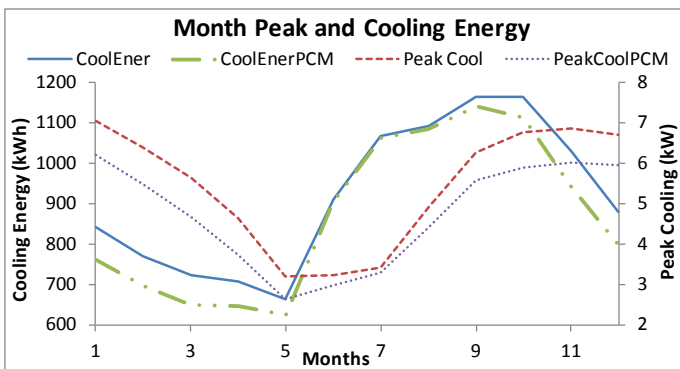| Variable	Value
% Weight of PCM in Insulation	40%
Equivalent Latent Heat	68 kJ/kg
Thermal Conductivity	0.0337 W/mK
Density	60 kg/m^3
Specific Heat	960 J/kg K
Thickness Wall	0.1m
Composite Latent Storage	270 kJ/m^2
Amount of PCM	1.6 kg/m^2

Figure 5. Predicted monthly peak and cooling energy for Case 600 building with (PeakCool, CoolEner) and without PCMs (PeakCoolPCM, CoolEnerPCM)

Figure 5 shows the predicted monthly cooling energy (left axis) and monthly peak cooling (right axis) for Case 600 building with and without PCMs with a nonlinear curve for Phoenix, Arizona. For both buildings, cooling energy increased during the summer as expected. Interestingly, annual peak cooling occurs in January (during winter) due to clear skies and

a large clear window area in the south wall that allows a large amount of solar radiation to enter the building. In addition, maximum peak cooling reduction and energy savings are not in summer but in winter as explained before, due to the outdoor temperature variable above and below the melting range.

Predicted percentage of annual PCM cooling energy savings were calculated comparing to the building without PCMs and are shown in Table 5. Among different PCM curves, predicted percentage of annual cooling energy savings were similar all within ±0.7% of the savings calculated from nonlinear PCM. In addition, annual peak cooling was not sensitive to different linearization. However, predicted monthly and hourly energy savings and peak reduction showed seasonal differences between linearization curves that in some cases were noteworthy.

Table 5. Predicted Annual Energy Savings and Peak Demand Reduction

Melting Profile	Annual Energy Savings	Peak Demand Reduction
NonLin	5.3%	11.9%
L-1	6%	11.9%
L-2	5.9%	12.1%
L-3	5.5%	12.0%
L-4	5.1%	11.9%
L-5	5.1%	11.8%
L-6	4.8%	11.6%

Figure 6 shows the predicted monthly energy savings associated with PCMs for all linearization cases with respect to the same building without PCMs. Figure 7 shows the corresponding peak reduction. For both graphs, the savings (kWh or kW) are represented in the left Y-axis and the percentage savings are in the right Y-axis. For the predicted monthly energy savings, linear curves L-1 and L-2 overestimate monthly energy savings up to 2% or 20kWh as shown in Figure 6. In contrast, the same curves, L-1 and L-2, tend to underestimate monthly peak reduction by up to 6% in August, as shown in Figure 7. In some cases, linear curve L-6 overestimated monthly peak reduction by up to 2%.
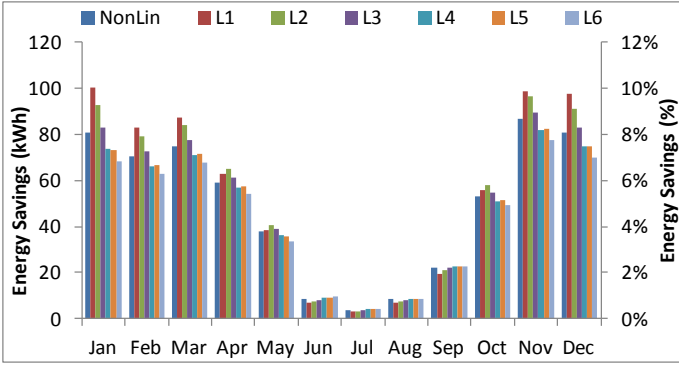
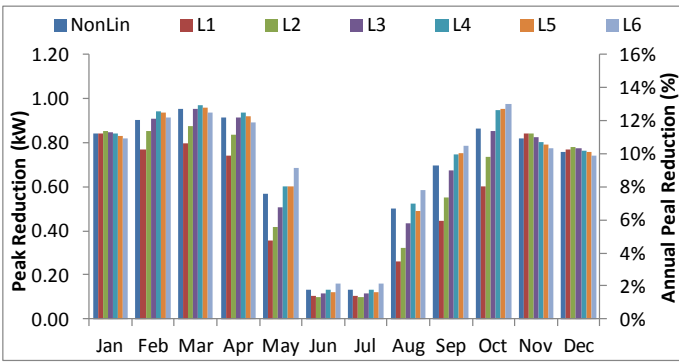Figure 6. Predicted monthly cooling energy savings (kWh and percentage) for different PCM linearization.

Figure 7. Predicted peak cooling reduction (kW and percentage) for different PCM linearization

Trends and differences between PCMs shown in Figure 6 and Figure 7 can be explained by looking at the hourly predicted cooling energy savings in Figure 8 through Figure 10 for August 22, March 2, and December 21. All PCMs used less cooling energy during the day with the highest savings around noon. Nevertheless, they use more cooling energy (negative savings) at the evening or at early morning than the building without PCMs due to the additional thermal storage. The time period of zero energy savings is due to low or no air conditioning use. The percentage of hourly differences between linear PCMs curves can be up to 20% by the introduction of a linear melting curve with an incorrect melting range. In summer (Figure 8), L-1 and L-2 underestimate the savings during the day by almost 20%. However the same PCMs overestimate the energy savings by more than 20% during spring (Figure 9) and winter (Figure 10) seasons. In addition, the effects of a wider melting range are more evident at the beginning or end of an air conditioning cycle. An opposite behavior is observed by the narrowest range L-6 but with a lesser magnitude of 10%. Likewise, L-1 and L-2 underestimate the negative energy savings at night. Overall, L-3 and L-4 obtained the closest agreement with respect to the non linear PCM results. Thus, this analysis shows that the initial annual and monthly performance showing smaller differences does not really represent the impact of replacing linear enthalpy curves for PCMs with nonlinear curves. The smaller difference is

mainly because the wider ranges tend to overestimate the thermal performance at some time while underestimating at a later time. Therefore, this reduces some of the larger variances shown in hourly analysis but eliminated in the larger time scales.
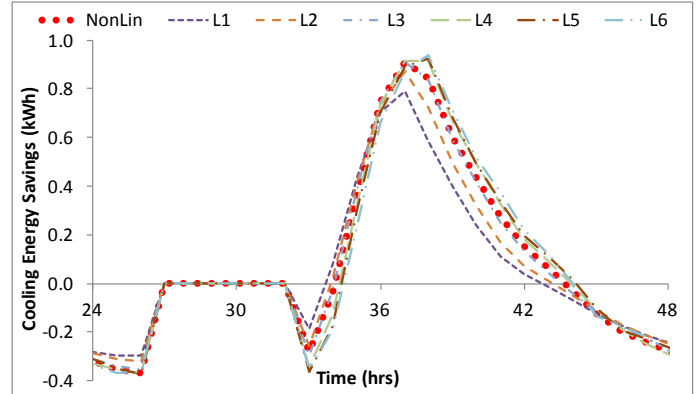

Figure 8. Predicted hourly cooling energy savings for all PCMs on August 22.
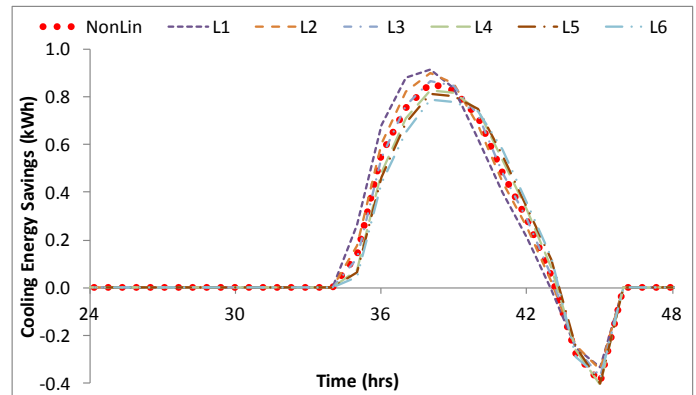

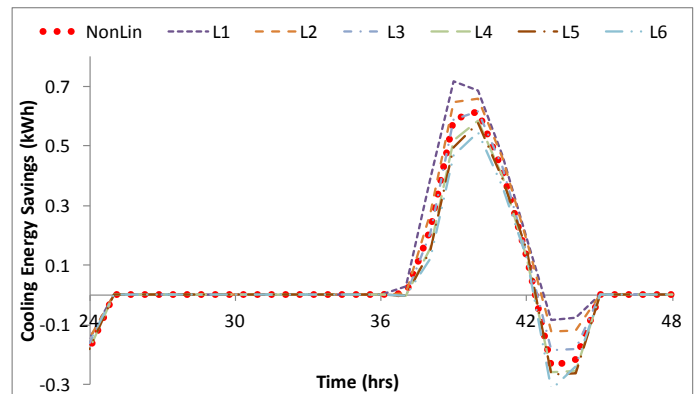Figure 9. Predicted hourly cooling energy savings for all PCMs on March 2.

Figure 10. Predicted hourly energy savings for all PCMs on December 21.

Predicted heating energy savings were also impacted by the linearization of the enthalpy curve. However, the predicted

annual heating energy for this particular climate and building represented about 5% of the total cooling energy. Figure 11 shows the predicted heating energy savings for the same day as Figure 10. Due to the controls of this building, weather, and the large south window, heating and cooling were necessary for several days. The results for the hourly heating savings show similar trends within the different PCMs; the widest melting ranges overestimate the energy savings while the narrowest melting range underestimates the energy savings. Predicted monthly heating energy savings are shown in Figure 12, depicting the same behavior as the hourly graph in Figure 11.
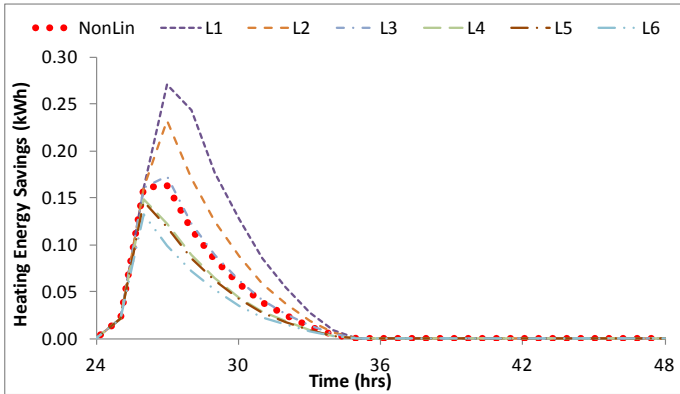

Figure 11. Predicted hourly energy savings for all PCMs on December 21
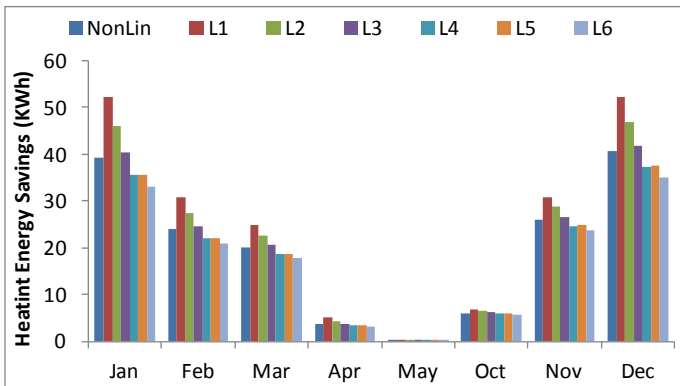

Figure 12. Predicted heating energy savings (kWh) for different PCM linear curves.

Figure 13 shows in the x-axis the normalized RMSE (from Table 1) of the six linear enthalpy curves. The left Y-axis shows the RMSE inside Heat Flux (Table 3) and right Y-axis shows the nonzero hourly RMSE Building Cooling Energy for the entire analyzed year. RMSE from the two tests shows similar trend and for both tests the best performance was L-3. In addition, the RMSE in the enthalpy curves is not necessary the best predictor of the error in the modeling results: the best two performers (L-3 and L-4) had the lowest RMSE, but one of the worst performers (L-2) has the third lowest RMSE. Future research will continue testing this idea.
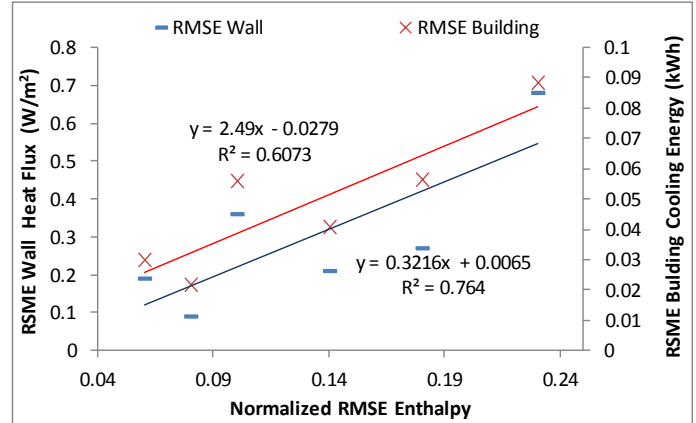

Figure 13. Normalized RMSE for the six linear enthalpy profiles (Table 1) vs the heat flux RMSE for the simple wall and the hourly RMSE cooling energy.

Overall, this analysis shows that it is possible to simplify the nonlinear behavior of PCM without sacrificing accuracy by using a linear enthalpy curve if a melting range covering roughly 80% of the latent heat is selected. For this specific example, using a linear enthalpy curve with a normalized RMSE (with the latent heat) of 0.06 to 0.08 show in all tests performed in this study the smallest difference with the results obtained with the nonlinear PCM. Future studies will test different PCM applications as well as enthalpy curves with more complex behavior.

CONCLUSIONS

This study analyzed the level of accuracy needed for PCM enthalpy curve to accurately simulate energy savings. This study analyzes the effects a nonlinear enthalpy profile has on thermal performance and expected energy benefits for PCM-enhanced insulation located in walls and attics. The impacts of accurately inputting realistic nonlinear enthalpy profile for PCMs versus simpler linear profiles is analyzed annually, monthly and hourly based on peak load reduction and energy savings using the Conduction Finite Difference (CondFD) algorithm in EnergyPlus. Annual energy savings show no major difference among the different linear curves versus the non-linear enthalpy curve. Although monthly and hourly results show that all PCMs followed the same profile, hourly analysis illustrates that if simpler linear profiles are used, users should try to specify a melting range covering roughly 80% of the latent heat. Otherwise, hourly results can differ by up to 20%. Specifically, close agreement between PCM linear profiles and realistic PCM was found when the normalized RMSE of the linear enthalpy profile was less than 0.08. The results for the hourly heating savings show similar trends within the different PCMs: using the entire melting range of the nonlinear enthalpy curve tends to overestimate the energy savings while excessively narrowing the melting range tends to underestimate the energy savings. Future studies will test different PCM

applications as well as enthalpy curves with more complex behavior.

NOMENCLATURE
PCM= Phase change materials
CondFD= Conduction Finite Difference
h = enthalpy
Cp = specific heat of material
T = temperature
ρ= density
Δx= space between nodes

$k_W = \frac{\left(k_{i+1}^{j+1}+k_i^{j+1}\right)}{2}$, thermal conductivity for interface between

i node and i+1 node

$k_E = \frac{\left(k_{i-1}^{j+1}+k_i^{j+1}\right)}{2}$, thermal conductivity for interface between i
node and i-1 node

$k_i = k\left(T_i^{j+1}\right)$, if thermal conductivity is variable
i = node being modeled
i+1 = node adjacent to interior of construction
i-1 = node adjacent to exterior of construction
j+1 = current time step
j = previous time step

ACKNOWLEDGMENTS

REFERENCES
1. Peippo, K., P. Kauranen, and P.D. Lund, "Multicomponent PCM wall optimized for passive solar heating," *Energy and Buildings,* 1991. 17(4): 259-270.
2. Stovall, T.K. and J.J. Tomlinson, 'What are the potential benefits of including latent storage in common wallboard?' *Journal of Solar Energy Engineering, Transactions of the ASME*, 1995. 117(4): 318-325.
3. Kosny, J., S. Shrestha, T. Stovall and D. Yarbrough, "Theoretical and Experimental Thermal Performance Analysis of Complex Thermal Storage Membrane Containing Bio-base Phase Change Material (PCM)," *Thermal Performance of the Exterior Envelopes of Whole Buildings XI International Conference.* 2010: Clearwater Beach, Florida p. 11.
4. Z Zhang, Y., K. Lin, Q. Zhang and H Di. "Preparation, thermal performance and application of shape-stabilized PCM in energy efficient buildings," *Energy and Buildings*, 2006. 38(10): 1262-1269.
5. Tabares-Velasco, P.C., C. Christensen, and M. Bianchi, "Simulated Peak Reduction and Energy Savings of Residential Building Envelope with Phase Change Materials", *ASHRAE Transactions*. 2012: San Antonio, TX. p. 8.
6. Heim, D. and J.A. Clarke, "Numerical modelling and thermal simulation of PCM-gypsum composites with ESP-r," *Energy and Buildings,* 2004. 36(8): 795-805.
7. Heim, D., "Isothermal storage of solar energy in building construction," *Renewable Energy*, 2010. 35(4): 788-796.
8. Schossig, P., et al., "Micro-encapsulated phase-change materials integrated into construction materials," S*olar Energy Materials and Solar Cells*, 2005. 89(2-3): p. 297-306.
9. Ibáñez, M., A. Lázaro, B. Zalba, and L.F. Cabeza. "An approach to the simulation of PCMs in building applications using TRNSYS," *Applied Thermal Engineering*, 2005. 25(11-12): 1796-1807.
10. Koschenz, M. and B. Lehmann, "Development of a thermally activated ceiling panel with PCM for application in lightweight and retrofitted buildings," *Energy and Buildings*, 2004. 36(6): 567-578.
11. Tabares-Velasco, P.C., C. Christensen, and M. Bianchi, "Verification and Validation of EnergyPlus Phase Change Material Model for Opaque Wall Assemblies," *Building and Environment*, 2012. 54: 186–196.
12. Tabares-Velasco, P.C. and B. Griffith, "Diagnostic test cases for verifying surface heat transfer algorithms and boundary conditions in building energy simulation programs," *Journal of Building Performance Simulation*, 2012 doi:10.1080/19401493.2011.595501.
13. Castellón, C., E. Gunther, H. Mehling, S. Hiebler and L. F. Cabeza, "Determination of the enthalpy of PCM as a function of temperature using a heat-flux DSC— A study of different measurement procedures and their accuracy," *International Journal of Energy Research*, 2008. 32(13): 1258-1265.
14. Günther, E., S. Hiebler, H. Mehling and R. Redlich, "Enthalpy of Phase Change Materials as a Function of Temperature: Required Accuracy and Suitable Measurement Methods," I*nternational Journal of Thermophysics*, 2009. 30(4): p. 1257-1269.
15. EnergyPlus, EnergyPlus Engineering Reference: The Reference to EnergyPlus Calculations. 2011, Ernest Orlando Lawrence Berkeley National Laboratory. p. 1130.
16. Shrestha, S., W. Miller, T. Stovall, A. Desjarlais, K. Childs, W. Porter, M. Bhandari and S Coley. "Modeling PCM-Enhanced Insulation System and Benchmarking EnergyPlus against Controlled Data Field," *Building Simulation 2011: 12th Conference of International Building Performance Simulation Association,* 2011. Sidney.
17. Kosny, J., S. Shrestha, D. Yarbrough, P. Childs, W. Miller, M. Bianchi, J. Smith, T. Fellinger, E. Kossecka

and E. Lee, "Theoretical and Experimental Thermal Performance Analysis of Building Shell Components Containing Blown Fiberglass Insulation Enhanced with Phase-Change Materials (PCM)," *Thermal Performance of the Exterior Envelopes of Whole Buildings XI International Conference*. 2010: Clearwater Beach, Florida. p. 13.